

Tactile Sensing-Based Control Architecture in Multi-Fingered Arm for Object Manipulation

Hanafiah Yussof, Masahiro Ohka, Hirofumi Suzuki, Nobuyuki Morisawa and Jumpei Takata

Abstract—This report presents the development of tactile sensing-based control architecture in a multi-fingered humanoid robot arm for object manipulation tasks. With the aim to enhance the ability to recognize and manipulate object in humanoid robot, we developed a novel optical three-axis tactile sensor system mounted on fingertips of the humanoid robot fingers. This tactile sensor applies an optical waveguide transduction method, and capable of acquiring normal and shearing force. Trajectory generation based on kinematical solutions at the arm and fingers, together with control system structure and sensing principle of the tactile sensor system are presented. We proposed control algorithm based on tactile sensing in the robot control system. Object manipulation experiments are conducted using hard and soft objects. Experimental results revealed that the proposed control system enable the finger system to recognize low force interactions based on tactile sensing information to grasp the object surface and manipulate it without causing damage to the object and the sensor elements.

Index Terms—Tactile sensing-based control architecture, optical three-axis tactile sensor, object manipulation, multi-fingered humanoid robot arm.

I. INTRODUCTION

In real application of humanoid robots in human environment, besides the capability of reliable navigation and obstacle avoidance, they are also required to performing certain tasks that need manipulation skills, such as finding and turning on switches, opening door knob or locks, removing objects, assembling, etc. As demonstrated by humans, handling and manipulating objects can support them to move around safely and effectively. Human environments present special challenge for robot manipulation since they are complex, dynamic, uncontrolled, and difficult to perceive reliably. Hence, robots need skills and suitable sensing system to realize contact sense with environments. This report presents development of control system architecture based on tactile sensing in a multi-fingered humanoid robot arm to enhance performance of object manipulation in humanoid robotics. We utilized an optical three-axis tactile sensor as the sensing device.

Hanafiah Yussof and Masahiro Ohka are with the Graduate School of Information Science, Nagoya University, Furo-cho Chikusa-ku Nagoya 464-8601 Japan (phone: +81-52-789-4251; fax: +81-52-789-4800; e-mail: Hanafiah: hanafiah@nuem.nagoya-u.ac.jp, Ohka: ohka@is.nagoya-u.ac.jp)

Hirofumi Suzuki and Nobuyuki Morisawa are with the Graduate School of Engineering, Nagoya University, Nagoya, Japan (e-mail: h_suzuki@nuem.nagoya-u.ac.jp, n_morisawa@nuem.nagoya-u.ac.jp)

Jumpei Takata is with the Olympus Corporation, Japan.

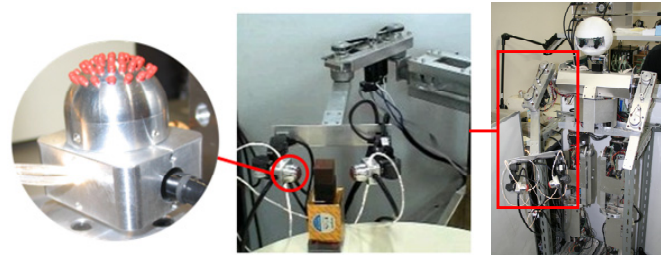


Fig. 1. Multi-fingered humanoid robot arm mounted with optical three-axis tactile sensors at fingertips.

The sense of touch or tactile sensing is the process of determining physical properties and events through contact with objects in the world. A tactile sensor system is essential as a sensory device to support the robot control system [1-3], particularly in object manipulation tasks. This tactile sensor is capable of sensing normal force, shearing force, and slippage, thus offering exciting possibilities for application in the field of robotics for determining object shape, texture, hardness, etc. However, tactile sensor is an especially appropriate sensing device that has too often been neglected in favor of vision based approaches. To date, while a great deal of research has been applied to the development of sensors especially visual and auditory sensors, comparatively little progress has been made with regards to sensors translating the sense of touch [3].

Research on tactile sensor is basically motivated by tactile sensing system of human skin. It is well known that human's tactile sense is very accurate and sensitive. Eventually, the most important distinction between the sensor types is between static and dynamics, in the sense that dynamics do not react to constant pressure. The dynamics sensors are of special importance for actively checking surface texture and properties, such as roughness, flatness, etc. Meanwhile, static sensors are more on improvement of imperfect grips.

In human, the skin structure provides mechanism to sense static and dynamics pressure simultaneously with extremely high accuracy. On the other hand, most tactile sensors developed nowadays are capable of detecting both static and dynamic pressure. Although accuracy and consistency are still remaining as main problems, the tactile sensing characteristic offers exciting possibilities for application in the field of robotics, especially for application in robotic finger or gripper system to perform object manipulation tasks [4][5]. Basically, in order to effectively perform the object manipulation tasks, the robotic systems required at least two types of tactile information: contact sense and slippage. Therefore, the tactile sensor system must be able to measure force in direction of

three axes. The contact sense is normally defined by measuring normal force, by means of static tactile sensing. Meanwhile, the slippage is defined by measuring shearing force, by means of dynamic tactile sensing.

In this research, we developed and analyze the performance of a novel optical three-axis tactile sensor system mounted on robotic fingers of a humanoid robot arm to conduct object manipulation tasks. Fig. 1 shows structure of the multi-fingered humanoid robot arm used in this research. It consists of two robotic fingers and the tactile sensors are mounted on each fingertip. In this report, at first we present the development of the optical three-axis tactile sensor. Secondly, we explain the structure and kinematical formulations of the multi-fingered humanoid robot arm, in which the tactile sensor is mounted on fingertips of each finger. This multi-fingered arm system is developed for experimental and evaluations of the tactile sensor system towards future application in real humanoid robot. Next, we explain control algorithm of the robotic fingers based on the tactile sensing information. Finally, we present experimental results of object manipulation tasks with soft and hard objects.

II. STATE-OF-THE-ART SURVEY OF TACTILE SENSING IN ROBOT MANIPULATION

Robot manipulation is fundamentally relies on contact interaction between the robot and the world [6]. As blind people convincingly demonstrate, tactile sensing alone can support extremely sophisticated manipulation. Unfortunately, many traditional tactile sensing technologies do not fit the requirements of robot manipulation in human environments due to lack of sensitivity, dynamic range and material strength.

Recent research in robot manipulation has been focusing in development of new tactile sensor that take advantage of advances in materials, microelectromechanical systems (MEMS), and semiconductor technology [7-9]. For instance, a research team at MIT have developed sensor with a protruding shape that allows them to easily make contact with the world from many directions in a similar way to the ridges of a human fingerprint or the hair on human skin. By measuring the deformation of the compliant dome, the sensors can estimate the magnitude and direction of applied forces with great sensitivity. This tactile sensor has been applied in a compliant hand of humanoid robot *Obrero* [10]. Another interesting example is the human skin-like combined sensor which offers extremely high-sensitivity with forces as low as 5mN can be detected. This sensor is suitable for determining dynamic tactile information in object exploration and has been tested with two-jar gripper [11].

Another interesting example is the skin-type conformable and scalable tactile sensor developed by a research team at Tokyo University [12][13]. The novelty of this tactile sensor includes connectivity, cuttability, and bendability, allowing for easy attachment to the robot body to realize whole-body movements. This tactile sensor has been applied in adult-size humanoid robot bodies. However, this tactile sensor seems unsuitable for use in object manipulation, particularly to define low force interaction and determine slippage sensation.

Obviously, tactile sensor offers exciting possibilities for application in the field of robotics for determining object shape, texture, hardness, etc. Humanoid robotics is one of the application areas in robotics that have generated the most interest presently in regards to tactile sensor applications. This is because humanoid robots are the type of robot that practically suitable to coexist with human because of its anthropomorphism, human friendly design and applicability of locomotion [14]. In fact, to effectively work in built-for-human environments, humanoid robot requires sensing device that can measure physical properties and recognize shapes of the given object through contact interaction, thus the robot can generate suitable trajectories to handle and manipulate the object. To date, many great efforts by robotic researchers have been reported related with development of tactile sensor systems that are compatible for use in humanoid robot platform [2][15][16]. However, there are serious issues exist in object manipulation which based on tactile sensing in humanoid robotics as followings:

- The robot must use low force interactions to explore the object surface without altering its physical properties or causing damage.
- During the manipulation task when suddenly the object's weight is changes, the robot will have trouble controlling the exact grasping pressure.
- The robot will rarely be able to control the exact angle at which its tactile sensor makes contact with the object.
- The last issue is related to mechanical structure and material strength; tactile sensor elements, which are normally made from soft and elastic materials such as silicon rubber, not robust enough to handle strong impact and pressure during object manipulation tasks

Therefore, besides the development of novel tactile sensor system that capable of precisely measuring normal and shearing forces, the development of precision control algorithm based on the tactile sensing information in the robot control system is very important. However, development of such control system and algorithm is very difficult because of hardware and computation problems.

In this report, we present development of control system architecture in multi-fingered humanoid robot arm which based on tactile sensing. The control system combines robotic control with tactile sensor control which provides normal and shearing forces data simultaneously to the robot control system. We utilized our newly developed optical three-axis tactile sensor mounted on fingertips of robotic fingers.

III. OPTICAL THREE-AXIS TACTILE SENSOR

Tactile sensor is a device that can measure a given property of an object or contact event through physical contact between the sensor and the object. To date, several basic sensing principles are commonly in use in tactile sensor, such as capacitive sensor, piezoelectrical sensor, inductive sensor, optoelectrical sensor and piezoresistive sensor [3][10].

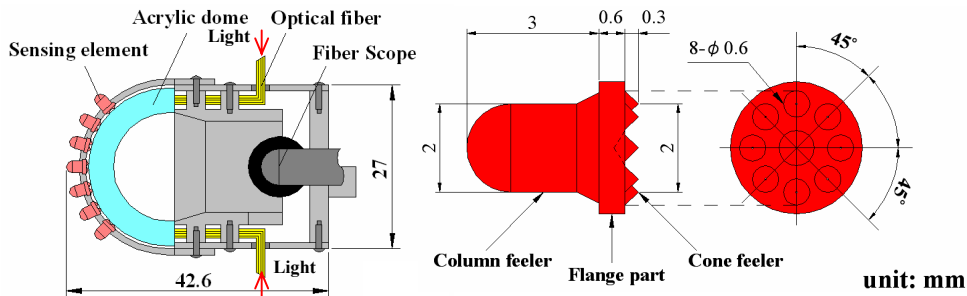


Fig. 2. Structure of optical three-axis tactile sensor and the sensing element.

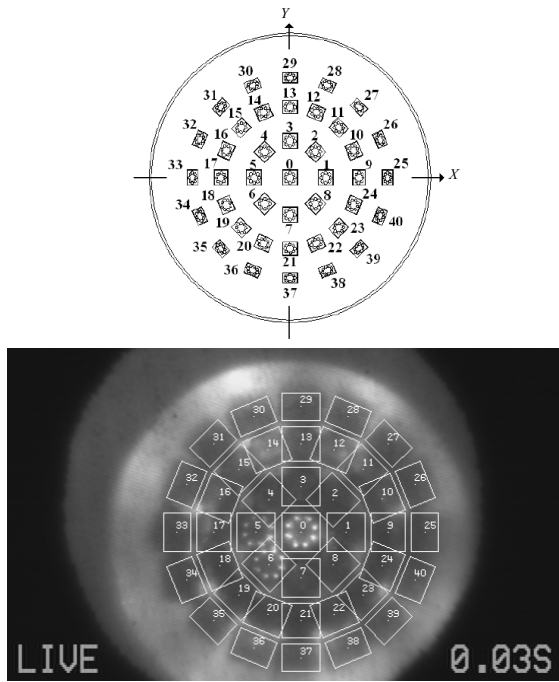


Fig. 3. Arrangement of sensing elements on fingertip and CCD camera-captured image of contact phenomenon in the tactile sensor.

In this research, with the aim of establishing object manipulation ability in real humanoid robot, we have developed an optical three-axis tactile sensor capable of acquiring normal and shearing force to mount on fingertips of humanoid robot arm. This tactile sensor is using optical waveguide transduction method, applying image processing techniques. This type of sensing principle is comparatively provides better sensing accuracy to detect contact phenomena from acquisition of three axial directions of forces, thus normal force and shearing force can be measured simultaneously [9]. The proposed three-axis tactile sensor has high potential compared to ordinal tactile sensor for fitting to a dextrose robotic arm.

The optical three-axis tactile sensor developed in this research is designed in a hemispherical dome shape consist of an array sensing elements. This shape is to mimic human fingertips structure for easy compliance with various shapes of objects. The hardware novelty consists of an acrylic hemispherical dome, an array of 41 peaces of sensing elements made from silicon rubber, a light source, an optical fibre-scope, and a CCD camera, as shown in Fig. 2. The silicone rubber sensing element that also indicated in this figure comprises one

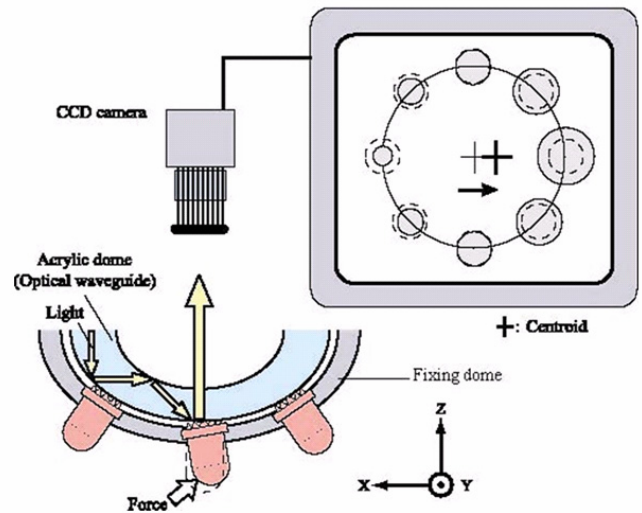


Fig. 4. Sensing principle of optical three-axis tactile sensor.

columnar feeler and eight conical feelers. The eight conical feelers remain in contact with the acrylic surface while the tip of the columnar feeler touches an object. The sensing elements are arranged on the hemispherical acrylic dome in a concentric configuration with 41 sub-regions as shown in Fig. 3.

The sensing principle of this tactile sensor is shown in Fig. 4. Referring to this figure, the light emitted from the light source is directed towards the edge of the hemispherical acrylic dome through optical fibres. When an object contacts the columnar feelers, resulting in contact pressure, the feelers collapse. At the points where the conical feelers collapse, light is diffusely reflected out of the reverse surface of the acrylic surface because the rubber has a higher reflective index.

The contact phenomena consisting of bright spots caused by the feelers collapse are observed as image data, which are retrieved by the optical fiber-scope connected to the CCD camera and are transmitted to the computer. The dividing procedure, digital filtering, integrated gray-scale value and centroid displacement are controlled on the PC using auto analysis program applying the image analysis software Cosmos32. In this situation, the normal force of F_x , F_y and F_z values are calculated using the integrated gray-scale value G , while shearing force is based on the horizontal centroid displacement. The displacement of the gray-scale distribution u is defined in (1), where i and j are orthogonal base vectors of the x - and y -axes of a Cartesian coordinate, respectively.

$$u = u_x i + u_y j \quad (1)$$

This equation is according to calibration experiments, whereby material functions are identified with piecewise approximate curves such as bi-linear and curves [16]. Consequently, each force component is defined in (2).

$$F_x = f(u_x), F_y = f(u_y), F_z = g(G) \quad (2)$$

IV. TRAJECTORY GENERATION IN MULTI-FINGERED HUMANOID ROBOT ARM

A. Humanoid Robot Arm

The humanoid robot arm developed in this research consists of 3-dofs: two dof (pitch and roll) at the shoulder and one dof (roll) at the elbow. The arm structure and control system was designed based on the earlier developed 21-dof humanoid robot Bonten-Maru II. However, some refinement and new modules have been added to comply with the robotic finger and tactile sensor system. Each joint is driven by a DC servomotor with a rotary encoder and a harmonic drive-reduction system, and is controlled by a PC with the Fedora Core Linux OS.

In the arm, upper link l_1 is connecting shoulder joints with elbow joint, while lower link l_2 connecting elbow joint with two robotic fingers. Trajectory generation of the arm is generated by determination of forward and inverse kinematics solutions. To describe translation and rotational relationship between adjacent joint links, we employ a matrix method proposed by Denavit-Hartenberg [17], which systematically establishes a coordinate system for each link of an articulated chain.

Figure 5 displays a model of the robot arm describing the configurations and orientation of each joint coordinates, and five sets of joint-coordinates frames. Consequently, corresponding link parameters of the arm can be defined as shown in Table 1. From the Denavit-Hartenberg convention, definitions of the homogeneous transform matrix of the link parameters can be described as in (3). This equation is initially used to obtain forward kinematics for the arm.

$${}^0_h \mathbf{T} = {}^0_1 \mathbf{T} {}^1_2 \mathbf{T} {}^2_3 \mathbf{T} {}^3_h \mathbf{T} \quad (3)$$

$$= \begin{bmatrix} s_1 c_{23} & -s_1 s_{23} & c_1 & s_1(l_1 c_2 + l_2 c_{23}) \\ s_{23} & c_{23} & 0 & l_1 s_2 + l_2 s_{23} \\ -c_1 c_{23} & c_1 s_{23} & s_1 & -c_1(l_1 c_2 + l_2 c_{23}) \\ 0 & 0 & 0 & l \end{bmatrix}$$

Consequently, the end-effector's orientation \mathbf{R}_{arm} with respect to the reference coordinate and the position of the end-effector \mathbf{P}_{arm} in regard to global axes P_x , P_y and P_z are shown in (4).

$${}^0_h \mathbf{R}_{arm} = \begin{bmatrix} s_1 c_{23} & -s_1 s_{23} & c_1 \\ s_{23} & c_{23} & 0 \\ -c_1 c_{23} & c_1 s_{23} & s_1 \end{bmatrix}, {}^0_h \mathbf{P}_{arm} = \begin{bmatrix} s_1(l_1 c_2 + l_2 c_{23}) \\ l_1 s_2 + l_2 s_{23} \\ -c_1(l_1 c_2 + l_2 c_{23}) \end{bmatrix} \quad (4)$$

Here, s_i , c_i , s_{ij} and c_{ij} are respective abbreviations of $\sin\theta_i$, $\cos\theta_i$, $\sin(\theta_i + \theta_j)$ and $\cos(\theta_i + \theta_j)$ where $(i, j=1,2,3)$. As understood from (3) and (4), a forward kinematics equation can be used to compute the Cartesian coordinates of the robot arm when the joint angles are known. However, in real-time applications it is more practical to provide the end-effector's

Table 1. Link parameters at humanoid robot arm.

Link	θ_{iarm}	d	α	l
0	$\theta_{1arm} - 90^\circ$	0	90	0
1	θ_{2arm}	0	-90	0
2	θ_{3arm}	0	0	l_1
3	0	0	0	l_2

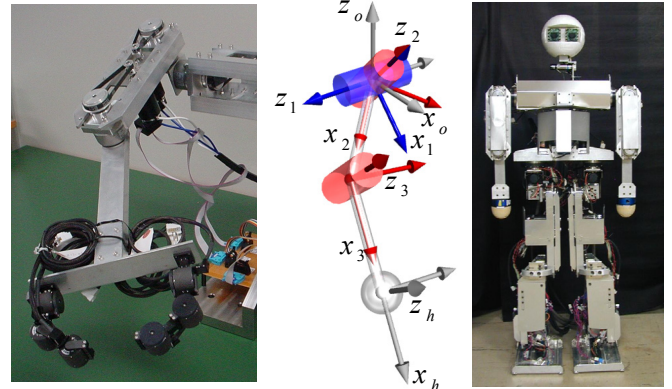


Fig. 5. Configuration of joint coordinates of the robot arm and appearance of the humanoid robot Bonyten-Maru II.

position and orientation data to the robot's control system than to define each joint angle that involved complicated calculations. Therefore, inverse kinematics solutions are more favorable.

To define joint angles θ_{1arm} , θ_{2arm} , θ_{3arm} in an inverse kinematics problem, at first each position element in (4) is multiplied and added to each other according to (5), which can also be arranged as in (6). Thus, θ_{3arm} is defined in (7).

$$P_{xarm}^2 + P_{yarm}^2 + P_{zarm}^2 = l_1^2 + l_2^2 + 2l_1 l_2 c_3 \quad (5)$$

$$c_3 = \frac{P_{xarm}^2 + P_{yarm}^2 + P_{zarm}^2 - (l_1^2 + l_2^2)}{2l_1 l_2} = C \quad (6)$$

$$\theta_{3arm} = \text{atan2}\left(\pm\sqrt{1-C^2}, C\right) \quad (7)$$

Consequently, θ_{3arm} is used to define θ_{2arm} , as shown in (8) ~ (12), where newly polar coordinates are defined in Eq. (10). Finally, θ_{1arm} can be defined as in (13).

$$k_1 = l_1 + l_2 c_3, \quad k_2 = -l_2 s_3 \quad (8)$$

$$p_{xz} = k_1 c_2 + k_2 s_2, \quad p_y = k_2 c_2 - k_1 s_2 \quad (9)$$

$$\phi = \text{atan2}(k_1, k_2) \quad (10)$$

$$\phi + \theta_{2arm} = \text{atan2}\left(\frac{p_{xz}}{r}, \frac{p_y}{r}\right) \quad (11)$$

$$= \text{atan2}(p_{xz}, p_y)$$

$$\theta_{2arm} = \text{atan2}(p_{xz}, p_y) - \text{atan2}(k_1, k_2) \quad (12)$$

$$\theta_{1arm} = \text{atan2}\left(\frac{p_x}{p_{xz}}, \frac{p_z}{p_{xz}}\right) \quad (13)$$

$$= \text{atan2}(p_x, p_z)$$

B. Robotic Fingers

The robotic finger system comprises of two articulated fingers as shown in Fig. 6. Each finger has 3-dof with micro-actuators (YR-KA01-A000, Yasukawa) is used in each joint. The micro-actuator consists of a micro AC servomotor, a harmonic gear and a digital encoder. The optical three-axis tactile sensor is mounted on each fingertip. Each joint connects to a PC via a motor driver and motor control board. The PC is installed with the Windows OS, and a Visual C++ compiler.

Trajectory generation of the fingers is defined by kinematical solutions derived by the same convention as the humanoid robot arm. According to the Denavit-Hartenberg notation, a model of the finger consist of configurations and orientation of each joint coordinates and five sets of joint-coordinates frames is shown in Fig. 6. The actuator angular velocity is derived by kinematics-based resolved motion rate control which commonly known as an algorithm for solving path-tracking problem in robotic control.

At this point, since joints angle of the finger are defined by kinematics solution as $\theta = [\theta_1, \theta_2, \theta_3]^T$, and put the fingertip moving velocity in global coordinate space as $\dot{r} = [\dot{x}, \dot{y}, \dot{z}]^T$, the joint rotation velocity at the finger is defined as following:

$$\dot{\theta} = J(\theta)^{-1} \dot{r}. \quad (14)$$

Here, inverse Jacobian matrix was employed to solve joint angle velocity which consequently satisfies the specified velocity vector \dot{r} of the fingertip in global coordinate plane. Initially, the Jacobian matrix is defined in (15).

$$J(\theta) = \begin{bmatrix} -R_{13}(l_2 + l_3 c \theta_2 + l_4 c \theta_{23}) & l_3(R_{11} s \theta_3 + R_{12} c \theta_3) + R_{12} l_4 & R_{12} l_4 \\ -R_{23}(l_2 + l_3 c \theta_2 + l_4 c \theta_{23}) & l_3(R_{21} s \theta_3 + R_{22} c \theta_3) + R_{22} l_4 & R_{22} l_4 \\ -R_{33}(l_2 + l_3 c \theta_2 + l_4 c \theta_{23}) & l_3(R_{31} s \theta_3 + R_{32} c \theta_3) + R_{32} l_4 & R_{32} l_4 \end{bmatrix} \quad (15)$$

Meanwhile, rotational transformation from the local frame of fingertip where tactile sensor is attached, to the frame of the workspace (refer Fig. 7) is calculated as follows:

$${}^0_s R = \begin{bmatrix} R_{11} & R_{12} & R_{13} \\ R_{21} & R_{22} & R_{23} \\ R_{31} & R_{32} & R_{33} \end{bmatrix} \begin{bmatrix} \cos 90^\circ & 0 & \sin 90^\circ \\ 0 & 1 & 0 \\ -\sin 90^\circ & 0 & \cos 90^\circ \end{bmatrix} = \begin{bmatrix} -R_{13} & R_{12} & R_{11} \\ -R_{23} & R_{22} & R_{21} \\ -R_{33} & R_{32} & R_{31} \end{bmatrix} \quad (16)$$

A direction cosine is obtained to estimate the slippage direction of the grasped object during object handling. The direction cosine of k -th sensing element in the local frame of the tactile sensor ($\alpha_k, \beta_k, \gamma_k$) is define in (17).

$$\begin{bmatrix} \alpha_k \\ \beta_k \\ \gamma_k \end{bmatrix} = \begin{bmatrix} \sin \theta_k \cos \phi_k \\ \sin \theta_k \sin \phi_k \\ \cos \theta_k \end{bmatrix}. \quad (17)$$

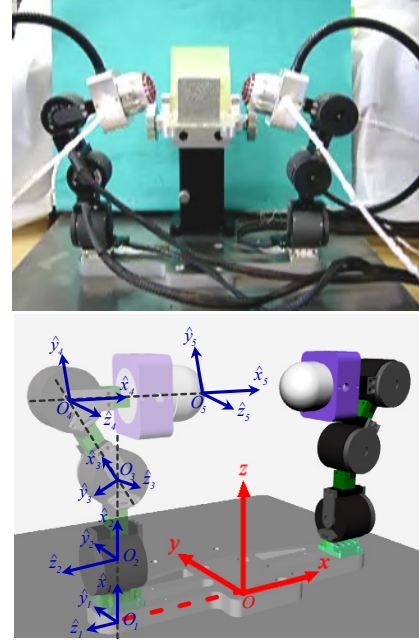


Fig. 6. Robotic fingers mounted with optical three-axis tactile sensor and configuration of joint coordinate frames at the finger.

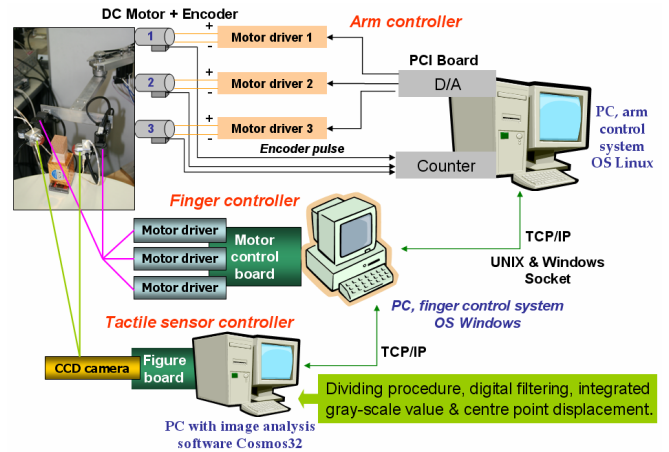


Fig. 7. Control system structure of multi-fingered humanoid robot arm with optical three-axis tactile sensor.

Hence, the direction cosine in the frame of workspace ($\alpha_{Gk}, \beta_{Gk}, \gamma_{Gk}$) is calculated as follows:

$$\begin{bmatrix} \alpha_{Gk} \\ \beta_{Gk} \\ \gamma_{Gk} \end{bmatrix} = \begin{bmatrix} -R_{13} & R_{12} & R_{11} \\ -R_{23} & R_{22} & R_{21} \\ -R_{33} & R_{32} & R_{31} \end{bmatrix} \begin{bmatrix} \sin \theta_k \cos \phi_k \\ \sin \theta_k \sin \phi_k \\ \cos \theta_k \end{bmatrix}. \quad (18)$$

V. CONTROL SYSTEM ARCHITECTURE

Figure 7 shows layout of the control system structure in the multi-fingered humanoid robot arm with robotic fingers and an optical three-axis tactile sensor. This system is comprised of three main controllers: arm controller, finger controller and tactile sensor controller. Each of these controllers is connected to each others using TCP/IP protocols via the internet. The arm controller consists of two main modules: robot controller and motion instructor. Shared memory is used to connect these two modules [18].

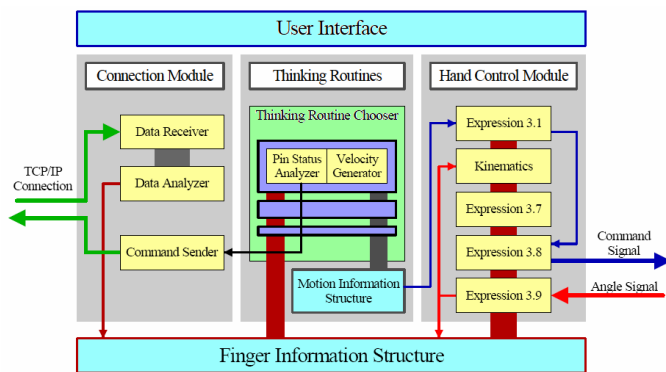


Fig. 8. Control system conception diagram of finger controller.

A. Finger Controller

The control system architecture of the robot finger controller is shown in Fig. 8. This controller is comprised of three modules: connection module, thinking routines, and hand/finger control module. It is connected with tactile sensor controller by the connection module using TCP/IP protocols. The most important considerations in controlling finger motions during performing object manipulation tasks are: what kind of information are acquired from the tactile sensor, how to translate and utilize this information, and how to send command to robot finger so that velocity of the finger motion can be control properly. These processes are performed inside the thinking routines module. As shown in Fig. 8, inside the thinking routines module, there is thinking routine chooser consists of pin status analyzer and velocity generator. Moreover, there is motion information structure which connecting to both pin status analyzer and velocity generator.

The pin status analyzer module is functioned to receive information from the tactile sensor about sensing elements condition, and use this information to decide suitable motion mode. Then it sends to the connection module a list of sensing elements that acquire tactile sensing information. Meanwhile, the velocity generator module is functioned to decide finger velocity based on finger information structure and motion information structure. The motion information structure consists of initial velocity, motion flag mode, etc, which is used to control finger movement. Meanwhile, finger information structure provides connection all modules so that they can share data of finger orientation, joint angle and tactile sensing data from each sensor elements.

User Interface was designed for the operator to provide commands to the finger control system. Finger control module controls the finger motion by calculating joints velocity and angle. In fact, this module can move finger without using sensing feedback. Thinking routines module receives tactile sensing data from tactile sensor and uses it to calculate fingertip velocity. In addition, to obtain low force interactions of the fingers during exploring object surface without causing damage, rotation velocity at each joint is defined precisely based on joint angle obtained in kinematics calculations, whereby force-position controls are performed.

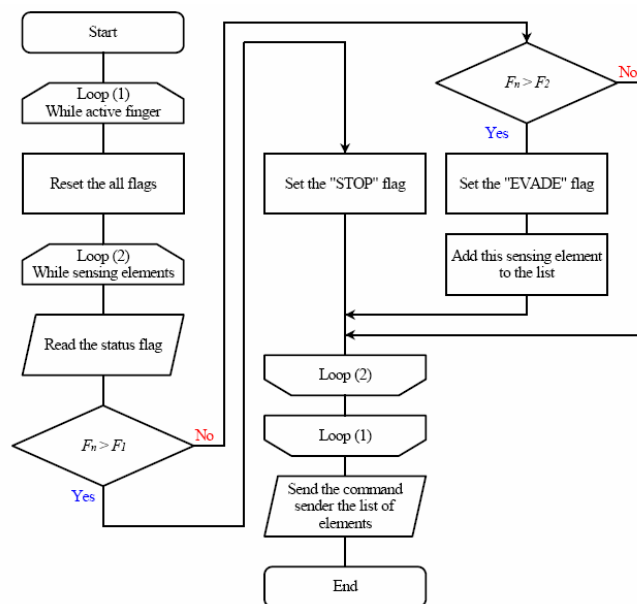


Fig. 9. Algorithm flowchart at the Pin Status Analyzer for case study.

To further understand about data communication process in the finger controller, we present a simple case study where finger touches an object and then avoid/evade the object by moving the finger to reverse direction. At first, the finger moving velocity to search for object is defined as V_0 . Next, we fix thresholds of normal force F_1 and F_2 . During searching process, when any of sensor elements touch an object, and if the detected normal force F_n is exceeding normal force threshold F_1 [N], the finger will stop moving.

Meanwhile, if the detected normal force F_n is exceeding threshold F_2 [N], the finger will move towards reverse direction of the sensing element that detects the highest force. At this moment the reverse velocity is defined as $|V_{re}|$. The parameters values of V_0 , F_1 , F_2 and $|V_{re}|$ are saved inside the motion information structure. The thresholds F_1 and F_2 are also delivered to sensor controller. When finger start moving, command to request status of each sensor elements are delivered to the sensor system according to control sampling phase of the finger system.

Detail of data communication process for the pin status analyzer and the velocity generator are shown in flowchart of Figs. 9 and 10, respectively. The processes at the pin status analyzer are explained as follows:

1. When sensor system received request command pin status analyzer, it will feedback status flag of each requested sensing element condition.
2. Connection module received the feedback data and then sends this data to the pin status analyzer, as well keeps it inside the finger information structure.
3. Pin status analyzer will then reset the finger motion ("STOP" and "EVADE") inside the motion information structure.
4. If the pin status analyzer received data flag that exceeds F_1 or F_2 , or both of them, it will list up the concerned sensor elements. The pin status analyzer will rise up

“STOP” flag if any listed sensor element is exceeded F_1 , meanwhile it will rise-up “EVADE” flag if any listed sensor element is exceeded F_2 . Then it sent the lists of data to the connection module.

5. The connection module will create a command to request normal force data of related sensor elements, and send the request to sensor system.
6. When sensor system received this request command, it will feedback normal force data of the requested sensor element to connection module at the finger controller.
7. Connection module received the feedback normal force data and then sends it to finger information structure. Based on this data, the velocity generator module will decide the velocity of the finger.

The processes at the Velocity Generator module are explained as follows:

1. If no flags “STOP” or “EVADE” rise-up, finger will move according to initial velocity V_0 .
2. If “STOP” flag is rise-up, finger velocity becomes 0.
3. If “EVADE” flag is rise-up, the finger will move towards reverse direction of the sensing element that detects the highest normal force value. To decide the finger velocity, when finger velocity is described as $V_r = (V_{rx}, V_{ry}, V_{rz})$, the direction cosine in the frame of workspace $(\alpha_{Gk}, \beta_{Gk}, \gamma_{Gk})$ is calculated as (19).

$$V_r = -|V_{re}| \begin{bmatrix} \alpha_{Gk} \\ \beta_{Gk} \\ \gamma_{Gk} \end{bmatrix} \quad (19)$$

Here, basically this generation of velocity is sent to hand/finger control module to solve Eq. (14). Therefore, controls of the finger based on tactile sensing information are conducted.

B. Sensor Controller

Figure 11 shows layout of tactile sensor controller. In the tactile sensor controller, based on image data captured by CCD camera, an image processing board Himawari PCI/S (Library Corp.) function as PCI bus picks up the image and sends it to internal buffer created inside the PC main memory. Sampling time for this process is 1/30 seconds. We use PC with Windows XP OS installed with Microsoft Visual C++. The image data are then sent to image analysis module applying Cosmos32 software which controls the dividing procedure, digital filtering, calculation of integrated gray-scale value and centroid displacement.

Since the image warps due to projection from a hemispherical surface, based on coordinate transformation of each sensing elements, the software Cosmos32 with auto image analysis program installed in the computer modifies the warped image data and calculates G , u_x and u_y to obtain the three-axis force applied to the tip of the sensing element. This enable the finger controller to perform force-position control to adjust grasp pressure of the two fingers on the given object.

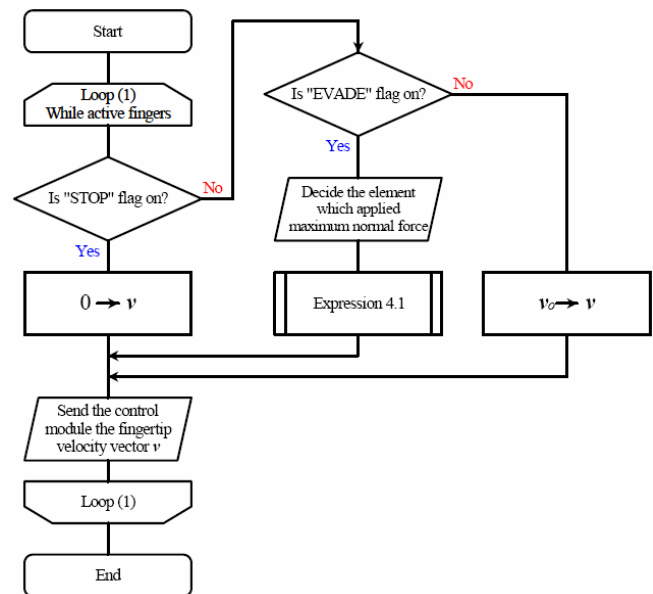


Fig. 10. Algorithm flowchart at the Motion Generator for case study.

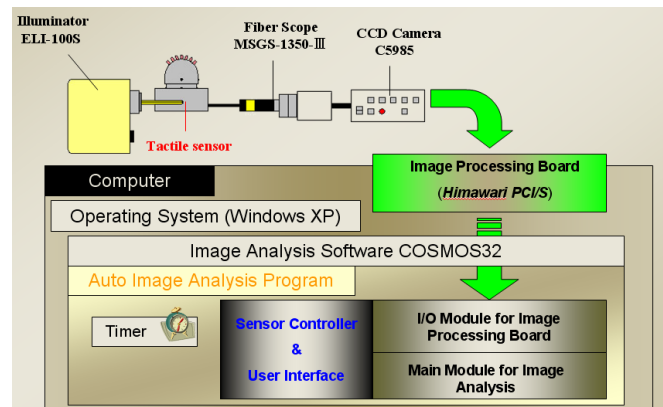


Fig. 11. Control system structure of optical three-axis tactile sensor.

VI. OBJECT MANIPULATION EXPERIMENT

The ability to sense hardness and/or softness will be particularly important in future applications to humanoid robot. Therefore, we have conducted this set of experiments in order to recognize and manipulate hard and soft object.

We used a cubic shape wood block represents a hard object, and a cubic shape thin paper box represents a soft object. Since the parameters of the human hand and fingers that are involved in sensing the hardness and/or softness of an object have not been fully researched, we conduct calibration test on the tactile sensor system to grasp objects with different hardness. This is to obtain basic data for estimation of optimum grasping. From the test results we estimate the force control parameters as shown in Table 2.

In this experiment, at first the two fingers grasp the object to define optimum gripping pressure. At this moment, the grasp pressure is controlled by parameters of normal force thresholds. Then both fingers lift up the object to z-axis direction while maintaining the optimum grasp pressure. During this motion, both normal pressure and slippage are concerned. Therefore the finger controller utilized parameters of normal force and

centroid change thresholds. Here, when shearing force exceeds the centroid change threshold, the finger's velocity for reinforcing the grasping pressure is calculated using (19), whereby vector velocity of the finger $v+\Delta v$ is defined by finger control module in the finger controller.

$$\Delta v = \begin{bmatrix} \alpha_{Gk} \\ \beta_{Gk} \\ \gamma_{Gk} \end{bmatrix} \quad (19)$$

Figure 12 shows photographs of the robot arm performing object manipulation with wood block. In this experiment, both fingers move along x -axis direction to grasp the wood block. When optimum grasping pressure is defined and the robot recognized the hardness of the object, both fingers lift up the wood block along y -axis, and then move forward along z -axis.

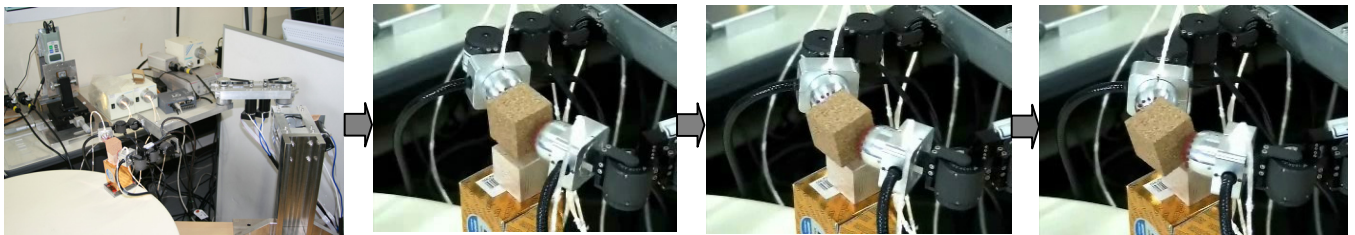


Fig. 12. Experiments of two robotic fingers manipulate wood block; lift up then move to forward direction.

Table 2. Parameters in experiments with hard and soft object.

Category	Sensor/Finger	Parameter
Interval for sampling	Finger	100ms/25ms
	Sensor	25ms
Threshold of normal force	F_1	0.5N
	F_2	1.8N
Threshold of centroid change	dr	0.004mm
Velocity of repush	v_p	2mm/s
Increment of normal force	ΔF	0.08N
Progress time	Δt	0.1s

Figures 13 and 14 show relation of normal and shearing forces detected with movements of fingers in xyz-axes for finger no.1. As shown in Fig. 13, the finger movement along x -axis is stop when the detected normal force exceeds threshold value of F_1 . Then it moves along y and z -axes while controlling grasping pressure based on the detected normal and shearing forces as shown in Figs. 13 and 14.

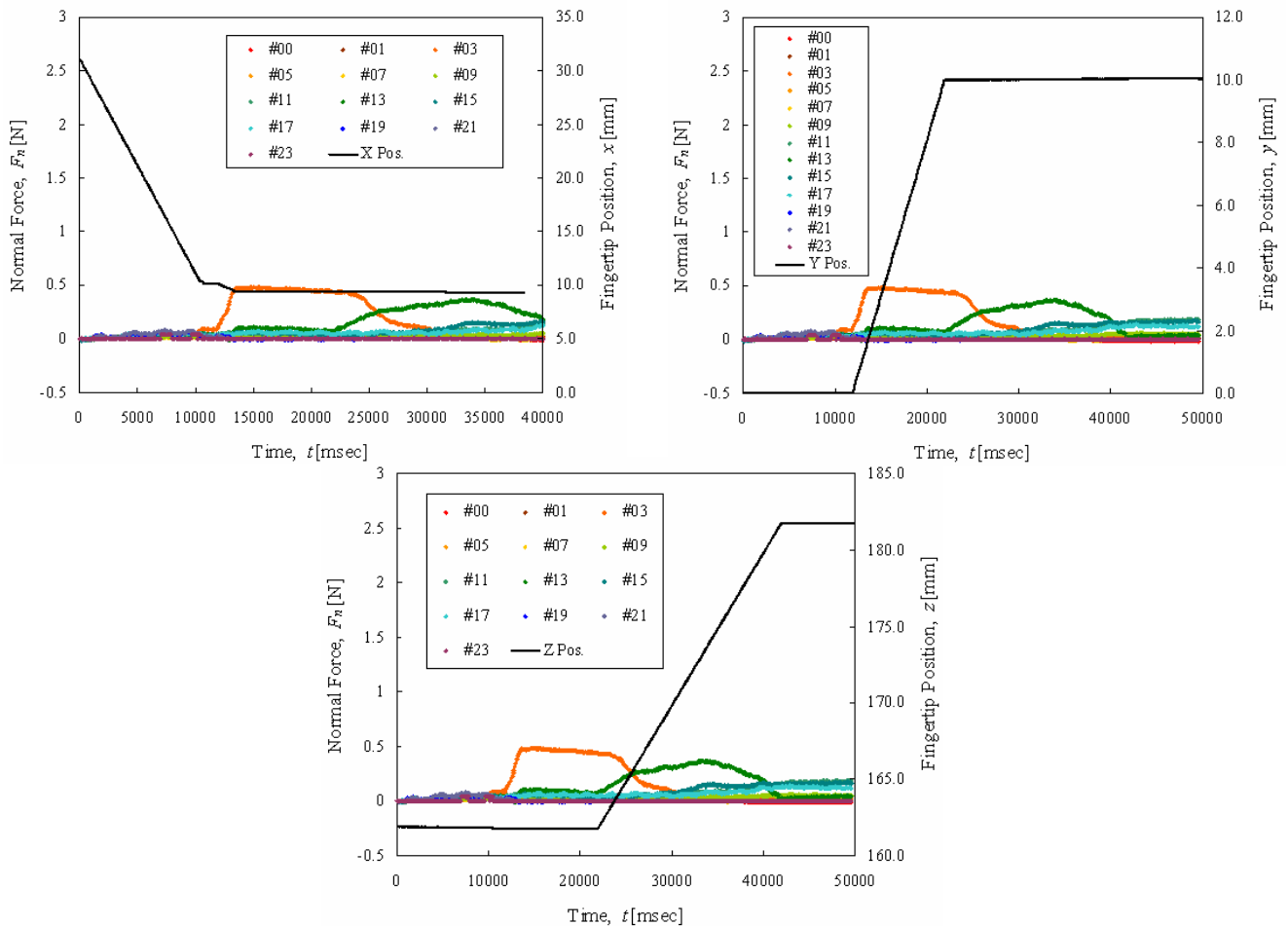


Fig. 13. Experiments of two robotic fingers manipulate wood block; normal force data for finger no. 1: (Left) Relation between normal force and fingertip movement at x -axis. (Middle) Relation between normal force and fingertip movement at y -axis. (Right) Relation between normal force and fingertip movement at z -axis.

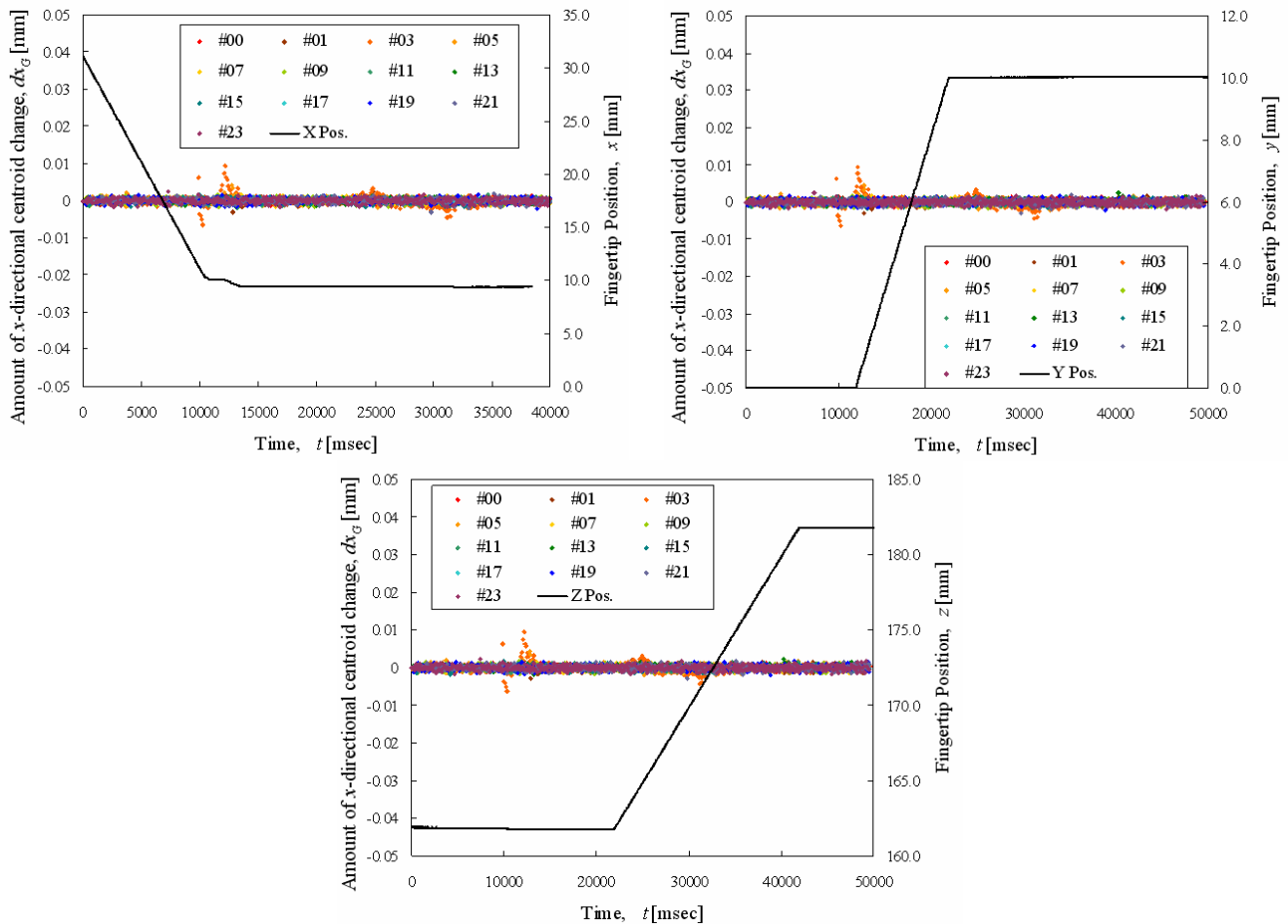


Fig. 14. Experiments of two robotic fingers manipulate wood block; shearing force data for finger no. 1: (Top-left) Relation between amount of x-directional centroid change and fingertip movement at x-axis. (Top-right) Relation between amount of x-directional centroid change and fingertip movement at y-axis. (Bottom) Relation between amount of x-directional centroid change and fingertip movement at z-axis.

Meanwhile, Fig. 15 shows photographs of the robot arm performing object manipulation with paper box. The cube-shaped paper box weight about 0.5 grams. The same control method was applied in the experiment with soft object. In this experiment, both fingers move along x -axis direction to grasp the paper box. When optimum grasping pressure is defined and the robot recognized the hardness of the object, both fingers lift up the wood block along y -axis. Then the fingers manipulate the paper box by performing motion like twisting the paper box. Consequently, relation of normal and shearing forces detected with movements of fingers in xyz -axes for both fingers are shown in Figs. 16, 17, 18, and 19, respectively.

Referring to these graphs, due to a very light weight of the paper box, the detected normal force is not exceeding minimum force parameter F_l , as shown in Figs. 16 and 17 for both fingers. Therefore, the grip pressure is controlled in regards to the detection of shearing force, as shown in Fig. 18 and 19 for both fingers, whereby threshold of centroid change was fixed at 0.004 mm. Based on the proposed control algorithm, the fingers maintains its grip on the object surface within optimum pressure without damaging the object. Finally, the robot fingers managed to perform twisting motion of the paper box without crushing it.

This experimental result shows that the proposed control algorithm is capable of preventing the probability of damaging a soft and light objects during handling tasks, that normally caused by overloading of grip pressure. In addition, this control scheme can be used to solve material strength problems of tactile sensor elements. This is because at first the fingers will performs soft touch on object surface in order to explore the object hardness before performing grasp and manipulation. When the robot control system realizes the object hardness condition, then the finger system can perform grasp and manipulation tasks safely by controlling grip force and re-push velocity on the object surface. This ensure the safety of tactile sensor elements which normally made by soft materials.

In both experiments, the fingers managed to grasp the objects within optimum grasp pressure, lift it to upwards direction, and then performed some movements manipulating the objects. The experimental results for both experiments revealed that the proposed control scheme managed to recognize low force interactions and define hardness distinction to grasp the object surface within optimum grasp pressure without causing damage to the object and the sensor elements. In addition, the formulations applied in this system enable precise control of the fingertips from determination of joint rotation angles and velocity.

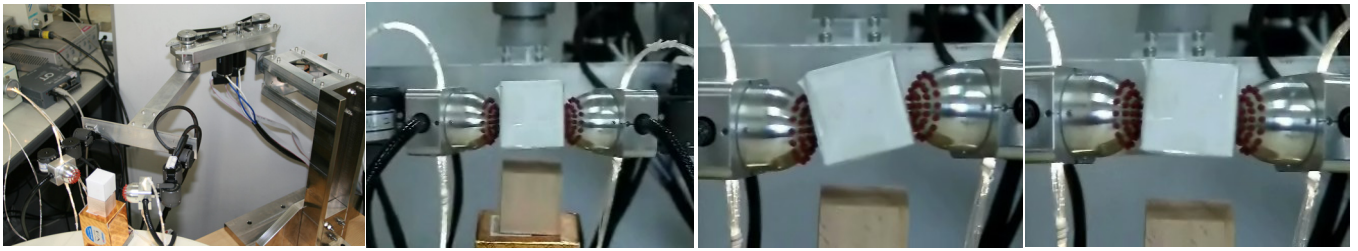


Fig. 15. Experiments of two robotic fingers manipulate paper box; lift up then twist the box.

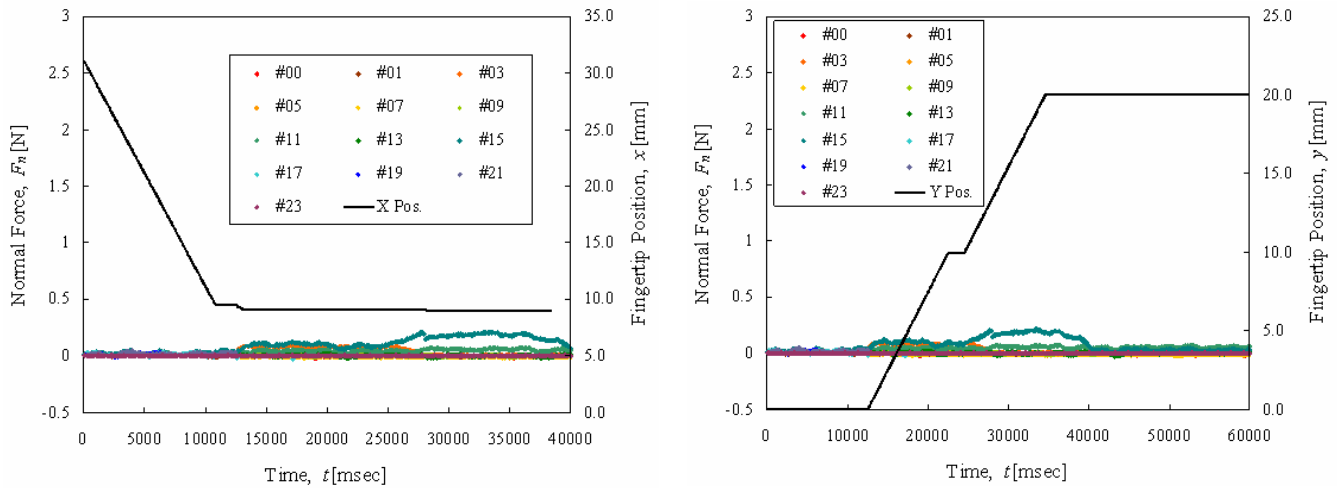


Fig. 16. Experiments of two robotic fingers manipulate paper box; normal force data for finger no. 1: (Left) Relation between normal force and fingertip movement at x-axis. (Right) Relation between normal force and fingertip movement at y-axis.

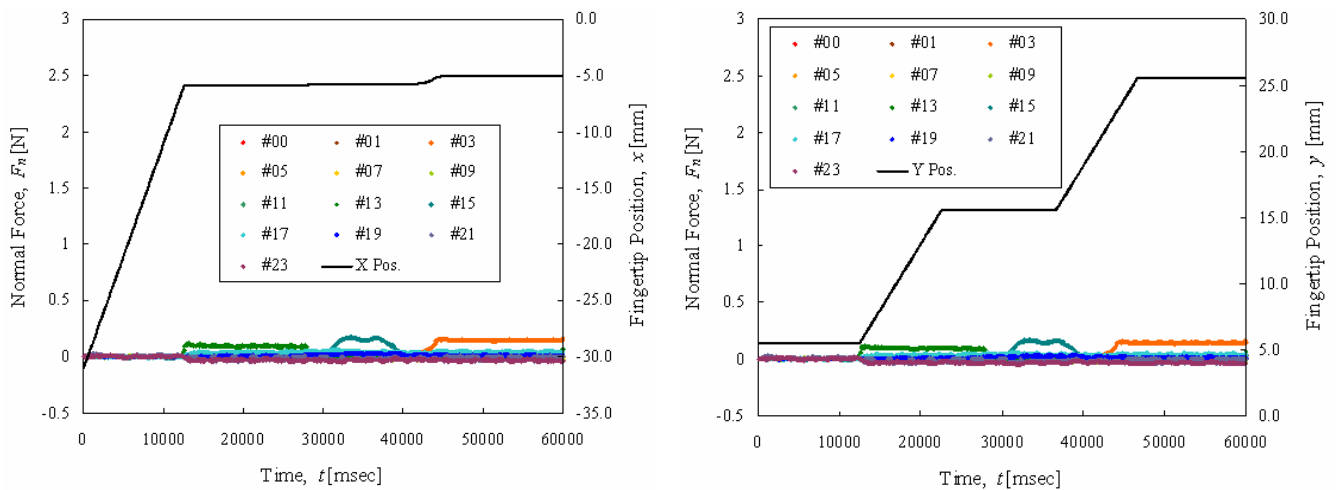


Fig. 17. Experiments of two robotic fingers manipulate paper box; normal force data for finger no. 2: (Left) Relation between normal force and fingertip movement at x-axis. (Right) Relation between normal force and fingertip movement at y-axis.

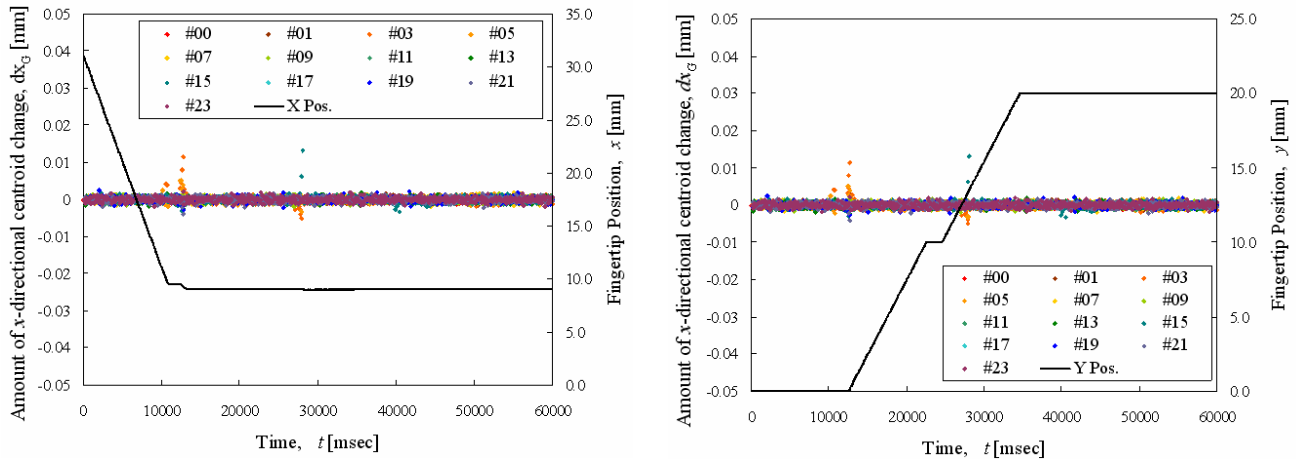


Fig. 18. Experiments of two robotic fingers manipulate paper box; shearing force data for finger no. 1: (Left) Relation between amount of x-directional centroid change and fingertip movement at x-axis. (Right) Relation between amount of x-directional centroid change and fingertip movement at y-axis.

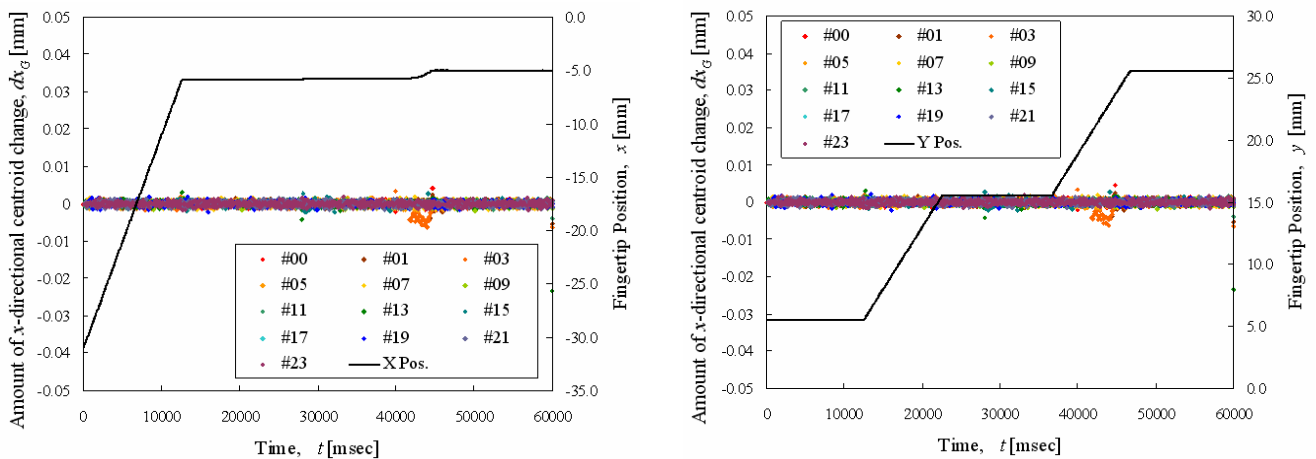


Fig. 19. Experiments of two robotic fingers manipulate paper box; shearing force data for finger no. 2: (Left) Relation between amount of x-directional centroid change and fingertip movement at x-axis. (Right) Relation between amount of x-directional centroid change and fingertip movement at y-axis.

VII. CONCLUSION

In this report, we presented the development of control system architecture based on tactile sensing in a multi-fingered humanoid robot arm for object manipulation tasks. We developed a novel optical three-axis tactile sensor system capable of acquiring normal and shearing force. The optical three-axis tactile sensor provided valuable tactile information for the robot control system to recognize contact interaction with objects. To generate trajectory of the robot arm and fingers, we present kinematical formulations based on coordinate transformation matrices derived by Denevit-Hartenberg convention.

We designed the robot control system architecture comprises of three main controllers: arm, finger and tactile sensor controller. The arm controller consists of two main modules: robot controller and motion instructor. Shared memory is used to connect these two modules. The finger controller is comprised of three modules: connection module, thinking routines, and hand/finger control module. The sensor controller is consists of a PC installed with an image analysis software

Cosmos32 and image processing board Himawari PCI/S. Each of these controllers is connected to each others using TCP/IP protocols via the internet. We proposed a new control algorithm in the robot control system based on tactile sensing data obtained by the optical three-axis tactile sensor.

To evaluate performance of the proposed system and algorithm, we conduct object manipulation experiment of hard and soft objects using the multi-fingered humanoid robot arm with optical three-axis tactile sensors are mounted on each fingertip. The robot fingers grasp the objects within optimum grasp pressure, lift it to upwards direction, and then performed some movements manipulating the objects. During experiments, normal and shearing forces data were compiled in graphs and we analyzed the performance of the proposed control system from relationship of fingertip movements with the detected forces. Experimental results revealed good performance of the robot fingers to recognize low force interactions to grasp and manipulate different hardness of objects. The fingers also managed to manipulate object without damaging it or the sensing elements.

In addition, this proposed control algorithm can be used to solve material strength problems of tactile sensor elements. This is because the fingers will perform soft touch on object surface in order to explore the object hardness before performing grasp and manipulation. It is anticipated that using this novel control scheme with tactile sensing technology will help advance the evolution of humans and robots working together in real life.

VIII. ACKNOWLEDGEMENTS

A part of this study was supported by fiscal 2006 Grant-in-Aid for Scientific Research in Exploratory Research from the Japan Ministry of Education, Culture, Sports, Science and Technology (Grant no. 18656079), and Grant-in-Research by Japan Society for the Promotion of Science (JSPS) for fiscal year 2008-2010.

REFERENCES

- [1] S. Omata, Y. Murayama and C.E. Constantinou, "Real time robotic tactile sensor system for determination of the physical properties of biomaterials", *J. Sensors and Actuators A*, 112(2-3), 2004, pp. 278-285.
- [2] O. Kerpa, K. Weiss and H. Worn, "Development of a flexible tactile sensor system for a humanoid robot", *Proceeding of IROS2003*, vol. 1, Oct. 2003, pp. 1-6, Las Vegas, USA.
- [3] M.H. Lee and H.R. Nicholls, "Tactile sensing for mechatronics: a state of the art survey", *Journal Mechatronics*, 9(1), 1999, pp. 1-31.
- [4] R. Zollner, T. Asfour and R. Dillmann, "Programming by demonstration: dual-arm manipulation tasks for humanoid robots", *Proceeding of 2004 IEEE/RSJ International Conference on Intelligent Robots and Systems (IROS 2004)*, vol. 1, 2004, pp. 479 – 484.
- [5] W. Bluethmann, R. Ambrose, M. Diftler, E. Huber, A. Fagg, M. Rosenstein, R. Platt, R. Grupen, C. Breazeal, A. Brooks, A. Lockerd, A. Peters, O. C. Jenkins, M. Mataric and M. Bugajska, "Building an autonomous humanoid tool user", *Proceedings of IEEE-RAS/RSJ International Conference on Humanoid Robots (Humanoids)*, 2004, Santa Monica, CA
- [6] A. Edsinger and C. Kemp, "Manipulation in human environments", *Proceeding of IEEE/RSJ International Conference on Humanoid Robotics (Humanoids06)*, 2006, Italy.
- [7] Jin-Seok Heo, Jong-Ha Chung and Jung-Ju Lee, "Tactile Sensor Arrays Using Fiber Bragg Grating Sensors", *International Journal of Sensor and Actuator*, vol. 126, issue 2, 2006, pp. 312-327.
- [8] S. Omata, Y. Murayama and C. E. Constantinou, "Real time robotic tactile sensor system for the determination of the physical properties of biomaterials", *Journal Sensor and Actuator A*, vol. 112, issue 2-3, 2004, pp. 278-285.
- [9] M. Ohka, Y. Mitsuya, Y. Matsunaga, and S. Takeuchi, "Sensing characteristics of an optical three-axis tactile sensor under combined loading", *Robotica*, vol. 22, 2004, pp. 213-221.
- [10] L. Natale and E. Torres-Jara, "A sensitive approach to grasping", *Proc. 6th International Conference on Epigenetic Robotics*, Sept. 2006, France.
- [11] P. A. Schmidt, E. Mael, and R. P. Wurtz, "A sensor for dynamic tactile information with applications in human-robot interaction and object exploration", *Journal Robotics & Autonomous Systems*, vol. 54, issue 12, Dec. 2006, pp. 1005-1014.
- [12] Y. Ohmura, Y. Kuniyoshi and A. Nagakubo, "Conformable and scalable tactile sensor skin for curved surfaces", *Proceeding International Conference on Robotics and Automation (ICRA2006)*, 2006, pp 1348-1353, Orlando, Florida
- [13] Y. Kuniyoshi, Y. Ohmura and K. Terada, "Embodied basis of invariant features in execution and perception of whole-body dynamic actions – knacks and focuses of roll-and-rise motion", *Journal Robotics and Autonomous Systems*, vol. 48, 2004, pp.189-201.
- [14] K. Hirai, M. Hirose, Y. Haikawa and T. Takenaka, "The development of Honda humanoid robot," *Proceeding of IEEE International Conference on Robotics and Automation (ICRA98)*, 1998, pp. 1321-1326.
- [15] Y. Hanafiah, M. Ohka, H. Kobayashi, J. Takata, M. Yamano and Y. Nasu "Contribution to the development of contact interaction-based humanoid robot navigation system: Application of an optical three-axis tactile sensor", *Proceeding of 3rd ICARA06*, Dec. 2006, pp. 63-68, Palmerston North, New Zealand.
- [16] M. Ohka, H. Kobayashi and Y. Mitsuya, "Sensing precision of an optical three-axis tactile sensor for a robotic finger", *Proceeding of 15th RO-MAN06*, Sept. 2006, pp. 220-225, United Kingdom.
- [17] J. Denavit and S. Hartenberg, "A Kinematic Notation for Lower-pair Mechanisms Based upon Matrices", *Journal of Applied Mechanics*, 1955, vol. 77, pp. 215-221.
- [18] H. Yussof, M. Ohka, J. Takata and M. A. Ayub, "Development of an optical three-axis tactile sensor with a 3-DOF robot arm towards application in humanoid robot," *Proceedings of the 1st International Conference on Control, Instrumentation, and Mechatronics (CIM'07)*, CDR, 2007, Johor, Malaysia